

LOWER OLEFINS SYNTHESIS IN FISCHER–TROPSCH PROCESS USING SUPPORTED IRON-CATALYSTS

Alin VINTILA^{1*}, Adrian TRIFAN², Ioan CALINESCU³

Different Fe catalysts have been synthesized both conventionally and by ultrasonic impregnation with different promoters (K, Mn) to obtain light olefins with high selectivity from the synthesis gas, avoiding excess CO₂ production and reducing CH₄ formation. The performance of proposed catalysts was analyzed and compared in terms of CO conversion, saturated hydrocarbons C₂-C₄ selectivity, unsaturated hydrocarbons C₂-C₄ selectivity, and unsaturated hydrocarbons C₂-C₄ yield, while varying the temperature in the range 250 – 350 °C. The influence of CO:H₂ molar ratio (1:1 and 1:2) was also observed.

Keywords: Fischer–Tropsch synthesis, light olefins, catalyst, ultrasound assisted processes

1. Introduction

The process used for the catalytic conversion of syngas (CO and H₂) to organic compounds, mainly hydrocarbons of various chain lengths, is called Fischer-Tropsch synthesis (FTS)[1].

The FTS is a promising non-petroleum alternative, by conversion of syngas, derived from natural gas, coal or biomass, can be obtained fuels [2], valued-added compounds such as aromatics [3], oxygenates [4] and olefins [5, 6].

The widely accepted predictive approach for determining the distribution of hydrocarbons selectivities in FTS, is the Anderson-Schulz-Flory (ASF) model, which expresses the formed hydrocarbons weight fraction (W_n) as a function of their respective carbon number (n) and chain growth probability factor (α), as seen in equation (1):

¹ PhD Student, Bioresources and Polymer Science Department, Faculty of Chemical Engineering and Biotechnologies, University POLITEHNICA of Bucharest, Romania and National Research & Development Institute for Chemistry and Petrochemistry ICECHIM, Bucharest, Romania, e-mail: vintila_alin_94@yahoo.com

² Assoc. Prof., Bioresources and Polymer Science Department, Faculty of Chemical Engineering and Biotechnologies, University POLITEHNICA of Bucharest, Romania, e-mail: adrian.trifan@upb.ro

³ Prof., Bioresources and Polymer Science Department, Faculty of Chemical Engineering and Biotechnologies, University POLITEHNICA of Bucharest, Romania, e-mail: ioan.calinescu@upb.ro

$$W_n = n(1 - \alpha)^2 \cdot \alpha^{n-1} \quad (1)$$

The maximum production of light hydrocarbons theoretically obtained according to the AFS distribution is about 60 %, achieved at α factors of 0.45.

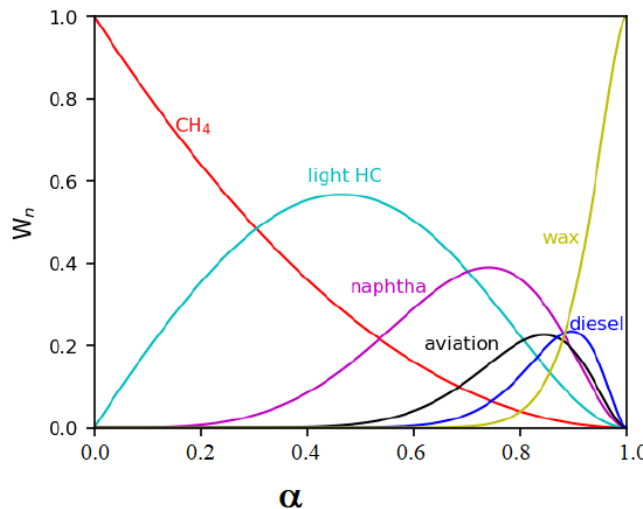


Fig. 1 ASF distribution as function of growth probability factor (α) according to equation (1) [1]

If the reaction conditions (temperature, molar ratio $\text{H}_2:\text{CO}$, pressure) are well chosen then the small hydrocarbon fraction may contain significant amounts of unsaturated hydrocarbons and the FTS can be considered a method of obtaining lower olefins.

The direct production of lower olefins, mainly ethylene, propylene and butylene, from syngas, is of significant interest among academic and industrial communities due to the widely applications of olefins as building blocks in the manufacturing of polymers and other products. [7]. Although traditionally olefins are obtained from petroleum sources through thermal or catalytic cracking [8], the diminishing reserves of petroleum shifted attention to the production of olefins from syngas derived from alternative raw materials [7, 9]. Among the pathways generally used in Fischer-Tropsch, the strategy of converting syngas to olefins (Fischer-Tropsch to olefins, FTO) is preferable over the cracking of liquid products and methanol or dimethyl ether to olefins synthesis (MTO/DMTO), having a lower energy demand and shorter reaction times [7, 10-15].

Catalyst development for direct conversion of CO-rich syngas to lower olefins is of great scientific and industrial interest [9], the hydrogenation of CO being a structure-sensitive reaction. Structural characteristics of the catalyst, among which exposed facets, particle size, and crystalline phase affect catalytic

performance [16]. The surface of the active phase is structurally dependant of various factors such as reaction conditions [17], supports [18], preparation methods [19], additives [20, 21], and reduction process [22]. For the selective production of light olefins iron-based catalysts have great potential, due to low-cost, high productivity in olefins, and low selectivity in methane [13], high resistance to contaminants, as well as the higher water-gas shift activity to promote the generation of H₂ enabling the in-situ adjustment of H₂:CO ratio [23, 24]. Product selectivity to light hydrocarbons can be achieved by carrying the FTO process at relatively high temperature, to benefit of the lower CH₄ selectivity of iron-based catalysts compared to other types of catalysts used in FT synthesis, such as Co and Ru [23, 25]. The need to fully understand and synthesized efficient iron-based catalysts for the FTO process led to a significant number of studies being published [6, 19, 25-28], with the consensus being that supported iron catalysts are better fitted for used in practice over unsupported catalysts, especially when α -Al₂O₃ and nanostructured carbon materials based supports are used, due to increased stability and homogeneous distribution of active sites [29-31].

Although the structure-sensitive nature of FTO on iron-based catalysts is well known [32, 33], the availability of information regarding catalytic performance due to particle size is limited, due to multiple factors affecting iron phase composition, including supports and promoters, and, in general, most catalysts that have been reported undergo deactivation [23, 28]. Both microstructure of active sites for syngas conversion and their physicochemical properties influence catalytic performance and are dependent by the preparation methods used [22].

The objective of the research was the synthesis (conventional and ultrasound assisted) and testing of iron catalysts with various promoters (K, Mn) and on different supports for the conversion of syngas to light olefins.

2. Experimental section

Reagents and experimental setup

Precursor reagents for catalysts and support preparation, of analytical purity were purchased from Merck, and they were used without further purification.

A series of catalysts were prepared in conventional, and ultrasound assisted processes, which were then used to carry out the Fischer-Tropsch synthesis (FTS) starting from hydrogen (H₂) and carbon monoxide (CO). Activation and testing of catalysts for FTS was performed with a Phoenix ThalesNano reaction system, which allows heterogeneous catalytic reactions to be

carried out at high pressures, up to 120 bar. The system was configured for gas phase reaction on a fixed catalyst layer.

The Phoenix enclosure provides temperature control in the two sections of metal reactor, which can be heated simultaneously with two independent metal blocks. The temperature difference between the two heating zones can be a maximum of 75 °C to ensure a good control of the temperature.

The gases N₂, H₂ and CO are supplied by the gas modules which allow control of the pressure (0-120 bar) and gas flows (0-100 mL/min) used in the reactions. To activate and regenerate the catalysts, a 1:1 molar ratio mixture of hydrogen and nitrogen, temperature of 400 °C and atmospheric pressure for 10 hours, were used.

To perform the FTS, the catalyst, about 0.5 g, was loaded to a metal reactor with an internal diameter of 3 mm. The length of the catalytic layer is 60 mm. To study its catalytic activity, the catalyst was used at low pressures (5 bar) and temperatures of 250-350 °C, and the CO: H₂ molar ratios used were 1:1 and 1:2. At each experimental point, at least three replicated samples were analyzed by on-line gas chromatography for a sufficiently long time, at least one hour, in order to assure that the reaction reached steady state.

The reaction mixture resulting from the FTS was analyzed through gas-chromatographic analysis, using a Buck Scientific 910 gas chromatograph (Buck Scientific Instruments, Norwalk, USA), the experimental conditions of the analysis are described by Sibianu et al. [34].

Catalyst preparation

Catalysts for FTS were prepared in conventional, and ultrasound assisted processes, using the wet impregnation method. Initially 10 g of support were loaded into a glass round-bottomed flask and heated at 80 °C for 30 min, under vacuum. The precursor salts were dissolved in distilled water under mixing, after which they were added to the flask containing the support. The impregnation process was carried out under vacuum using a rotavap to slowly evaporate the water at 50 °C and 100 rpm, with the temperature being raised to 80 °C in the last hour. For the conventional process a water bath is used for heating, while for the ultrasound assisted process, an ultrasonic bath is used instead. Following the impregnation step, the prepared catalysts were dried at 60 °C for 12 h, then calcinated for 4 h at 600 °C.

Calculation of conversions, selectivities and yields in FTS

Conversions, selectivities and yields were calculated by processing the primary data - the areas of the compounds in the gas chromatographic analysis, using the equations (2-5), provided below, where X represents the specific

compound for which the calculations are being carried out. The products were identified by comparison of the retention times with that of the individual compounds (CO, CO₂, methane, ethane, ethene, propane, propene, butane, butene, isobutane, isobutene).

*TOTAL moles of CO = unreacted moles of CO + moles of CO₂ + moles methane + 2 * moles of ethane + 2 * moles of ethene + 3 * moles of propane + 3 * moles of propene + 4 * moles of butane + 4 * moles of isobutene*

(2)

$$\text{Conversion CO (\%)} = \frac{\text{TOTAL moles CO} - \text{unreacted CO moles}}{\text{TOTAL moles CO}} * 100 \quad (3)$$

$$\text{Selectivity (X) (\%)} = \frac{\text{moles X}}{\text{TOTAL moles CO} - \text{unreacted CO moles}} * 100 \quad (4)$$

$$\text{Yield X (\%)} = \text{Conversion (\%)} * \text{Selectivity (X)} \quad (5)$$

3. Results and discussion

Catalytic activity

The activation/reduction of the catalysts was carried out at 400 °C for 10 h, under a 80 mL/min flow of hydrogen: nitrogen mixture with a ratio of 1:1. Catalyst activation was performed to reduce metal oxides to metals. The catalyst was employed in FTS at different temperatures and CO:H₂ molar ratios in order to investigate its catalytic activity. The working temperatures were 250 °C, 300 °C, 325 °C, 350 °C and the CO:H₂ molar ratio for each temperature set were 1:1 and 1:2.

At each temperature and molar ratio, several gas samples were collected in order to make sure that the chemical reaction achieves steady state. In order to observe the catalyst stability in the FTS, two series of catalytic tests were run, one after the catalyst activation and the other after the catalyst had been used in the FTS.

A proposed direction for improving the performance of iron-based catalysts, is the development of formulations consisting of other metals alongside iron. As seen from Fig. 2, a good performance was achieved by the potassium-manganese modified catalyst, with 80 % conversion of monoxide while maintaining a good selectivity towards unsaturated hydrocarbons. Even though the zinc-potassium-manganese catalyst had consistently higher selectivities towards olefins over the other studied catalysts, which in turn saw a sharp decrease in selectivity as the temperature increased, the main drawback for this catalyst is the low conversion rate. The best yields in unsaturated hydrocarbons are obtained on the Fe₁₅K₁Mn₁-Al₂O₃ catalyst.

When looking at the influence of the support on the activity of the $\text{Fe}_{25}\text{K}_1\text{Mn}_1$ based catalysts (Fig. 3), we observed that significantly higher conversion rates were achieved for the alumina and zeolite supported catalysts, especially when higher temperatures were used. The highest selectivity towards unsaturated hydrocarbons was reached by the zeolite supported catalyst, at 250 °C, with the main drawback being the low conversion rate. As the conversion rates increase with temperature, both alumina and zeolite supported catalysts favor the formation of saturated hydrocarbons. The best yields in unsaturated hydrocarbons are obtained on the alumina support.

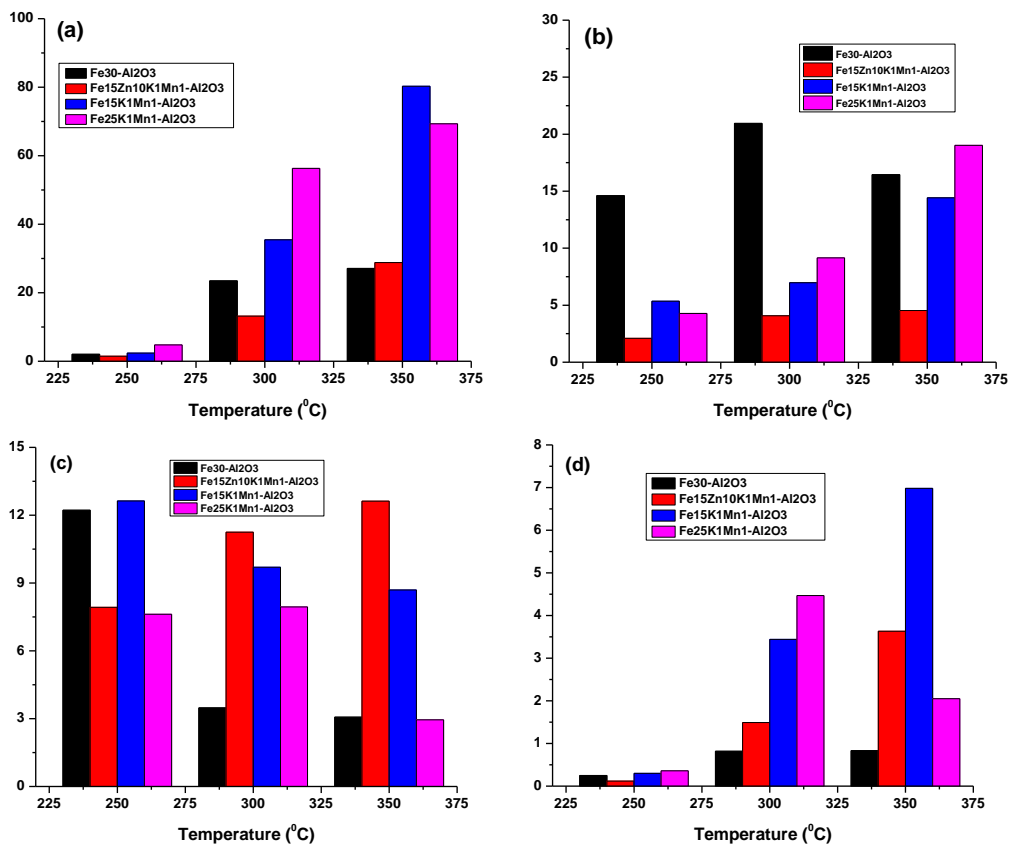


Fig. 2 Influence of composition on catalysts activity at 2:1 H_2/CO molar ratio; (a)-CO conversion; (b)-saturated hydrocarbons C₂-C₄ selectivity; (c)- unsaturated hydrocarbons C₂-C₄ selectivity; (d)- unsaturated hydrocarbons C₂-C₄ yield

Two types of catalysts have been proposed to study the influence of ultrasound during their preparation, specifically $\text{Fe}_{15}\text{K}_1\text{Mn}_1$ and $\text{Fe}_{15}\text{Zn}_{10}\text{K}_1\text{Mn}_1$, both supported on alumina (Fig. 4). In the first case, the use of ultrasound led to a decrease in catalytic activity with overall lower conversion rates regardless of the

temperatures used, and no significant changes in selectivity towards the compounds of interest. For the $\text{Fe}_{15}\text{Zn}_{10}\text{K}_1\text{Mn}_1$ catalyst, the inclusion of ultrasound during the impregnation step, allowed for higher conversion rates over the control sample, and increased selectivity towards saturated rather than unsaturated hydrocarbons.

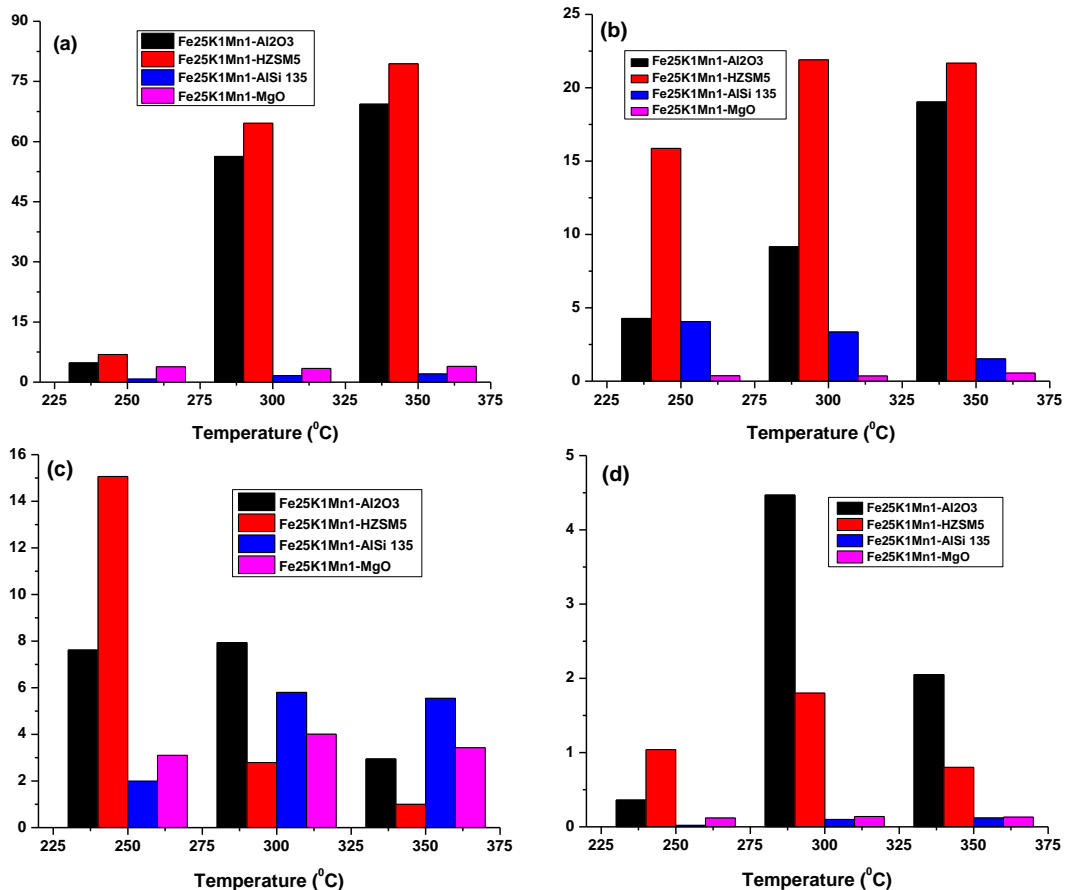


Fig. 3 Influence of support on catalysts activity at 2:1 H_2/CO molar ratio; (a)-CO conversion; (b)- saturated hydrocarbons C₂-C₄ selectivity; (c)- unsaturated hydrocarbons C₂-C₄ selectivity; (d)- unsaturated hydrocarbons C₂-C₄ yield

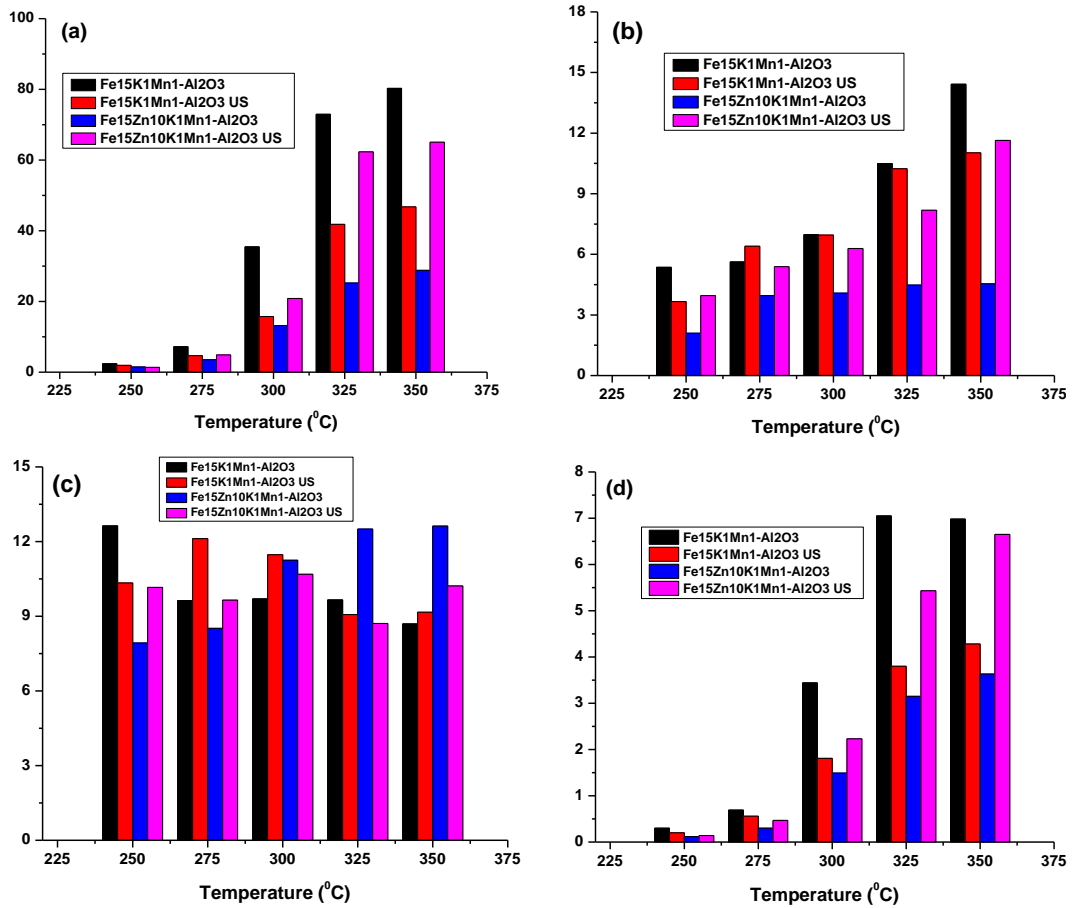


Fig. 4 Comparison of conventional and ultrasound assisted catalyst preparation method using 2:1 H₂/CO molar ratio; (a)-CO conversion; (b)-saturated hydrocarbons C₂-C₄ selectivity; (c)-unsaturated hydrocarbons C₂-C₄ selectivity; (d)-unsaturated hydrocarbons C₂-C₄ yield

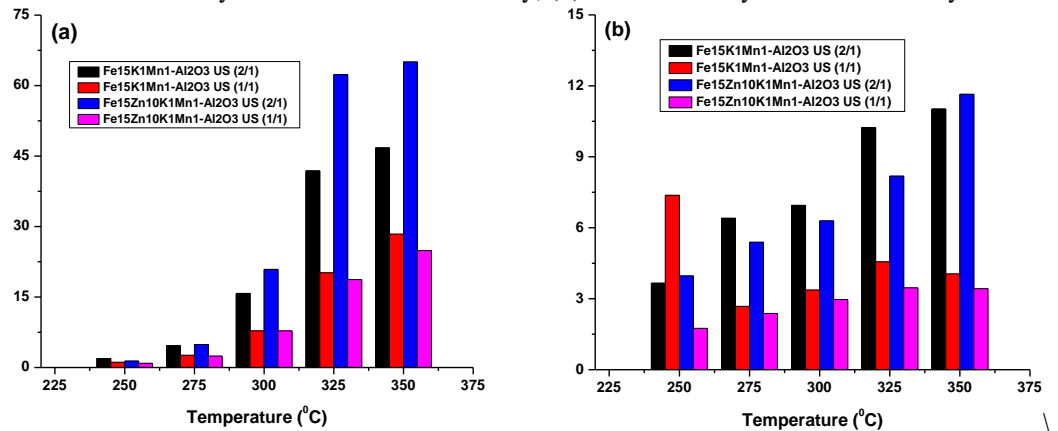


Fig. 5. Influence of H₂/CO molar ratio on catalysts activity: (a)-CO conversion; (b)-saturated hydrocarbons C₂-C₄ selectivity

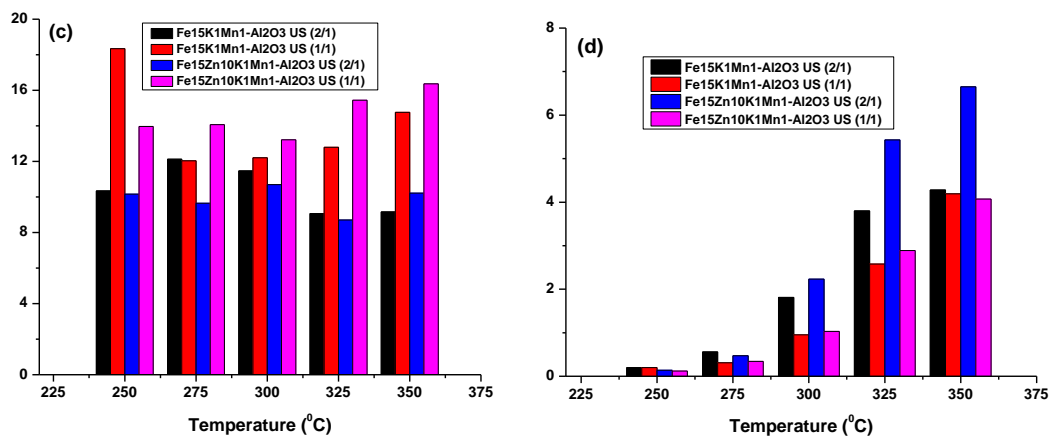


Fig. 5'. Influence of H_2/CO molar ratio on catalysts activity: (c)- unsaturated hydrocarbons $\text{C}_2\text{-}\text{C}_4$ selectivity; (d)- unsaturated hydrocarbons $\text{C}_2\text{-}\text{C}_4$ yield

Increasing the H_2/CO molar ratio from 1/1 to 2/1 (Fig. 5), led to a 2-fold increase in conversion rates for both $\text{Fe}_{15}\text{K}_1\text{Mn}_1$ and $\text{Fe}_{15}\text{Zn}_{10}\text{K}_1\text{Mn}_1$ catalysts, with a decrease in selectivity towards unsaturated hydrocarbons. The presence of excess hydrogen, besides moving the equilibrium towards the formation of products, and therefore higher yields, it also led to an increase in saturated hydrocarbons, most likely as a result of secondary hydrogenation reactions of the unsaturated hydrocarbons.

4. Conclusions

The results presented in this work demonstrated the improvement of the catalytic activity of iron-based catalysts during FTS, resulting in higher yields in prepared unsaturated hydrocarbons. Experimental data obtained have shown the ability of certain metal ions, combined potassium-manganese in particular, to enhance performance by integrating them in established formulations for iron based catalysts. The addition of ultrasound during the catalyst preparation phase yielded beneficial results for some catalyst, in terms of conversion rates and products of interest selectivities, suggesting that the use of ultrasound should be taken into consideration. The catalyst support used should also be considered, with alumina supported catalysts performing better than other proposed support materials, being also the preferred support for other experiments carried out in this study. Increasing the ratio of hydrogen to CO used, while improving conversion rates, in some cases almost doubling them, also favoured secondary hydrogenation reactions with the formation of saturated hydrocarbons, therefore a compromise between high conversion rates and high yields in the products of interest should be considered.

R E F E R E N C E S

1. <https://www.etipbioenergy.eu/biomass-to-liquids-btl-via-fischer-tropsch-a-brief-review> - accessed on 28.02.2022.
2. Y. An, Y. Zhao, F. Yu, T. Lin, Y. Lu, S. Li, Z. Li, Y. Dai, X. Wang, H. Wang, L. Zhong, and Y. Sun, Morphology control of Co2C nanostructures via the reduction process for direct production of lower olefins from syngas. *Journal of Catalysis*, 2018. **366**: p. 289-299.
3. Y. Xu, D. Liu, and X. Liu, Conversion of syngas toward aromatics over hybrid Fe-based Fischer-Tropsch catalysts and HZSM-5 zeolites. *Applied Catalysis A: General*, 2018. **552**: p. 168-183.
4. T. Lin, X. Qi, X. Wang, L. Xia, C. Wang, F. Yu, H. Wang, S. Li, L. Zhong, and Y. Sun, Direct production of higher oxygenates by syngas conversion over a multifunctional catalyst. *Angewandte Chemie International Edition*, 2019. **58**(14): p. 4627-4631.
5. K. Gong, T. Lin, Y. An, X. Wang, F. Yu, B. Wu, X. Li, S. Li, Y. Lu, L. Zhong, and Y. Sun, Fischer-Tropsch to olefins over CoMn-based catalysts: effect of preparation methods. *Applied Catalysis A: General*, 2020. **592**: p. 117414.
6. X. Gao, J. Zhang, N. Chen, Q. Ma, S. Fan, T. Zhao, and N. Tsubaki, Effects of zinc on Fe-based catalysts during the synthesis of light olefins from the Fischer-Tropsch process. *Chinese Journal of Catalysis*, 2016. **37**(4): p. 510-516.
7. W. Zhou, K. Cheng, J. Kang, C. Zhou, V. Subramanian, Q. Zhang, and Y. Wang, New horizon in C1 chemistry: breaking the selectivity limitation in transformation of syngas and hydrogenation of CO₂ into hydrocarbon chemicals and fuels. *Chemical Society Reviews*, 2019. **48**(12): p. 3193-3228.
8. G.F. Froment, Thermal cracking for olefins production. Fundamentals and their application to industrial problems. *Chemical Engineering Science*, 1981. **36**(8): p. 1271-1282.
9. H.M. Torres Galvis and K.P. de Jong, Catalysts for production of lower olefins from synthesis gas: a review. *ACS Catalysis*, 2013. **3**(9): p. 2130-2149.
10. B. Shi, Z. Zhang, B. Zha, and D. Liu, Structure evolution of spinel Fe-MII (M=Mn, Fe, Co, Ni) ferrite in CO hydrogenation. *Molecular Catalysis*, 2018. **456**: p. 31-37.
11. J. Bao, G. Yang, Y. Yoneyama, and N. Tsubaki, Significant advances in C1 catalysis: highly efficient catalysts and catalytic reactions. *ACS Catalysis*, 2019. **9**(4): p. 3026-3053.
12. J. Li, Y. Hou, Z. Song, C. Liu, W. Dong, C. Zhang, Y. Yang, and Y. Li, Chemical and structural effects of strontium on iron-based Fischer-Tropsch synthesis catalysts. *Molecular Catalysis*, 2018. **449**: p. 1-7.
13. B. Chen, X. Zhang, W. Chen, D. Wang, N. Song, G. Qian, X. Duan, J. Yang, D. Chen, W. Yuan, and X. Zhou, Tailoring of Fe/MnK-CNTs composite catalysts for the Fischer-Tropsch synthesis of lower olefins from syngas. *Industrial & Engineering Chemistry Research*, 2018. **57**(34): p. 11554-11560.
14. B. Gu, V.V. Ordomsky, M. Bahri, O. Ersen, P.A. Chernavskii, D. Filimonov, and A.Y. Khodakov, Effects of the promotion with bismuth and lead on direct synthesis of light olefins from syngas over carbon nanotube supported iron catalysts. *Applied Catalysis B: Environmental*, 2018. **234**: p. 153-166.
15. Y. Cheng, J. Lin, T. Wu, H. Wang, S. Xie, Y. Pei, S. Yan, M. Qiao, and B. Zong, Mg and K dual-decorated Fe-on-reduced graphene oxide for selective catalyzing CO hydrogenation to light olefins with mitigated CO₂ emission and enhanced activity. *Applied Catalysis B: Environmental*, 2017. **204**: p. 475-485.
16. W. Chen, T. Lin, Y. Dai, Y. An, F. Yu, L. Zhong, S. Li, and Y. Sun, Recent advances in the investigation of nanoeffects of Fischer-Tropsch catalysts. *Catalysis Today*, 2018. **311**: p. 8-22.

17. Y. An, T. Lin, F. Yu, X. Wang, Y. Lu, L. Zhong, H. Wang, and Y. Sun, Effect of reaction pressures on structure–performance of Co2C-based catalyst for syngas conversion. *Industrial & Engineering Chemistry Research*, 2018. **57**(46): p. 15647-15653.
18. X. Wang, W. Chen, T. Lin, J. Li, F. Yu, Y. An, Y. Dai, H. Wang, L. Zhong, and Y. Sun, Effect of the support on cobalt carbide catalysts for sustainable production of olefins from syngas. *Chinese Journal of Catalysis*, 2018. **39**(12): p. 1869-1880.
19. K. Mai, T. Elder, L.H. Groom, and J.J. Spivey, Fe-based Fischer Tropsch synthesis of biomass-derived syngas: effect of synthesis method. *Catalysis Communications*, 2015. **65**: p. 76-80.
20. Z. Li, T. Lin, F. Yu, Y. An, Y. Dai, S. Li, L. Zhong, H. Wang, P. Gao, Y. Sun, and M. He, Mechanism of the Mn promoter via CoMn spinel for morphology control: formation of Co2C nanoprisms for Fischer–Tropsch to olefins reaction. *ACS Catalysis*, 2017. **7**(12): p. 8023-8032.
21. Z. Li, L. Zhong, F. Yu, Y. An, Y. Dai, Y. Yang, T. Lin, S. Li, H. Wang, P. Gao, Y. Sun, and M. He, Effects of sodium on the catalytic performance of CoMn catalysts for Fischer–Tropsch to olefin reactions. *ACS Catalysis*, 2017. **7**(5): p. 3622-3631.
22. H.-S. Na, J.-O. Shim, S.-Y. Ahn, W.-J. Jang, K.-W. Jeon, H.-M. Kim, Y.-L. Lee, K.-J. Kim, and H.-S. Roh, Effect of precipitation sequence on physicochemical properties of CeO₂ support for hydrogen production from low-temperature water-gas shift reaction. *International Journal of Hydrogen Energy*, 2018. **43**(37): p. 17718-17725.
23. H.M. Torres Galvis, J.H. Bitter, T. Davidian, M. Ruitenbeek, A.I. Dugulan, and K.P. de Jong, Iron particle size effects for direct production of lower olefins from synthesis gas. *Journal of the American Chemical Society*, 2012. **134**(39): p. 16207-16215.
24. Z. Yang, S. Guo, X. Pan, J. Wang, and X. Bao, FeN nanoparticles confined in carbon nanotubes for CO hydrogenation. *Energy & Environmental Science*, 2011. **4**(11): p. 4500-4503.
25. K. Cheng, V.V. Ordomsky, B. Legras, M. Virginie, S. Paul, Y. Wang, and A.Y. Khodakov, Sodium-promoted iron catalysts prepared on different supports for high temperature Fischer–Tropsch synthesis. *Applied Catalysis A: General*, 2015. **502**: p. 204-214.
26. Y. Cheng, J. Lin, K. Xu, H. Wang, X. Yao, Y. Pei, S. Yan, M. Qiao, and B. Zong, Fischer–Tropsch synthesis to lower olefins over potassium-promoted reduced graphene oxide supported iron catalysts. *ACS Catalysis*, 2016. **6**(1): p. 389-399.
27. J. Lu, L. Yang, B. Xu, Q. Wu, D. Zhang, S. Yuan, Y. Zhai, X. Wang, Y. Fan, and Z. Hu, Promotion effects of nitrogen doping into carbon nanotubes on supported iron Fischer–Tropsch catalysts for lower olefins. *ACS Catalysis*, 2014. **4**(2): p. 613-621.
28. Y. Liu, J.-F. Chen, and Y. Zhang, The effect of pore size or iron particle size on the formation of light olefins in Fischer–Tropsch synthesis. *RSC Advances*, 2015. **5**(37): p. 29002-29007.
29. X. Zhou, J. Ji, D. Wang, X. Duan, G. Qian, D. Chen, and X. Zhou, Hierarchical structured α -Al₂O₃ supported S-promoted Fe catalysts for direct conversion of syngas to lower olefins. *Chemical Communications*, 2015. **51**(42): p. 8853-8856.
30. D. Wang, X. Zhou, J. Ji, X. Duan, G. Qian, X. Zhou, D. Chen, and W. Yuan, Modified carbon nanotubes by KMnO₄ supported iron Fischer–Tropsch catalyst for the direct conversion of syngas to lower olefins. *Journal of Materials Chemistry A*, 2015. **3**(8): p. 4560-4567.
31. X. Duan, D. Wang, G. Qian, J.C. Walmsley, A. Holmen, D. Chen, and X. Zhou, Fabrication of K-promoted iron/carbon nanotubes composite catalysts for the Fischer–Tropsch synthesis of lower olefins. *Journal of Energy Chemistry*, 2016. **25**(2): p. 311-317.

32. J. Xie, H.M. Torres Galvis, A.C.J. Koeken, A. Kirilin, A.I. Dugulan, M. Ruitenbeek, and K.P. de Jong, Size and promoter effects on stability of carbon-nanofiber-supported iron-based Fischer–Tropsch catalysts. *ACS Catalysis*, 2016. **6**(6): p. 4017-4024.
33. J. Xie, J. Yang, A.I. Dugulan, A. Holmen, D. Chen, K.P. de Jong, and M.J. Louwerse, Size and promoter effects in supported iron Fischer–Tropsch catalysts: insights from experiment and theory. *ACS Catalysis*, 2016. **6**(5): p. 3147-3157.
34. I. Sibianu, D. Berger, C. Matei, and I. Calinescu, Microwave assisted Fischer - Tropsch synthesis at a atmospheric pressure. *Revista de Chimie*, 2017. **68**: p. 1040-1043.